An analytical study for debonding in single-lap shear test by considering the residual strength

Available online at www.sciencedirect.com

ScienceDirect

Procedia Structural Integrity 33 (2021) 982–988

Structural Integrity Procedia

www.elsevier.com/locate/procedia

IGF26 - 26th International Conference on Fracture and Structural Integrity

An Analytical Study for Debonding in Single-lap Shear Test by Considering the Residual Strength

A. M. Mirzaei*, A. Sapora, M. Corrado, P. Cornetti

Department of Structural Engineering and Geotechnics, Politecnico di Torino, Corso Duca degli Abruzzi 24, 10129 Torino, Italy

Abstract

External bonding of composite reinforcements has become an accepted method for strengthening the existing structures, e.g., FRCM to concrete. In the present manuscript, the shear lag model is combined with two different bond-slip laws to investigate the mechanics of debonding of composite-to-substrate joints by considering the residual strength. Boundary conditions of the problem are written based on a so-called pull-push test, while the obtained equations can also be used for the pullout test. Results illustrate the considerable effect of friction in mode II debonding, even at starting the process. Despite the simplicity of equations and differences in bond-slip laws, it is demonstrated that both the models predict the debonding load with reasonable accuracy. Finally, some simple expressions – generalizing the ones without residual friction – are proposed to calculate the effective bond length.

Keywords: Mathematical modeling; Debonding; FRCM; Shear lag model; Residual strength; Direct shear test.

1. Introduction

Applying external plates to an existing structure is a possible way to enhance the load bearing, and it has become a popular technique, nowadays. On the other hand, for Fiber Reinforced Polymers (FRP), properties like high strength to weight ratio, as well as accessible and quick application seem promising while high thermal mismatch between the structure and epoxy resins as well as poor fire resistance are their drawbacks. To address these issues, Fiber-Reinforced

* Corresponding author. Tel.: +39 011 090 5312; Fax: +39 011 090 4899.
E-mail address: amir.mirzaei@polito.it

10.1016/j.prostr.2021.10.108

Cementitious Matrixes (FRCMs) were introduced. For this strengthening technique, one of the common problems is debonding of the reinforcement from the structure. It can be said that the direct shear test (or, in another name, pull-push test) is the most common experimental test to study the debonding of such structures, Fig. 1. Under this loading condition, it can be assumed that the interface is mainly subjected to shear, and we can ignore the effect of peeling stress, as it was shown that contribution of peeling stress is highly localized for this test (Muñoz-Reja et al., 2020). On the other hand, the one-dimensional shear-lag model (Volkersen, 1938) is a simple yet powerful approach for 1D analysis of structures as it was successfully applied to a considerable number of studies in the Literature (e.g., Grande et al., 2018). In this paper, the shear-lag model is employed by two different constitutive interface models to study the debonding of the reinforcement from the substrate by considering the effect of the residual strength, a feature which is necessary to take into account for the FRCM strengthening system. It is seen that during the experimental testing of the direct shear test of FRCM, the load-displacement curve does not fall to zero but to a constant value, due to the friction between the two components. In this paper, the influence of friction in the debonding behavior is considered as traction, therefore, it is called residual strength. In the following, a brief review on analytical solutions for debonding of the reinforcement from the structure in the direct shear test is provided.

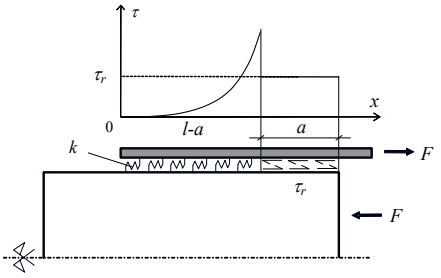

Fig. 1. A schematic view of the debonding process for the pull-push test.

Yuan et al. (Yuan et al., 2004), Cornetti and Carpinteri (Cornetti and Carpinteri, 2011), and Biscaia et al. (Biscaia et al., 2016) employed a bilinear, linear-exponential, and exponential interface softening law to study debonding behavior of FRP-to-concrete joints. A trilinear bond-slip law by taking the effect of the residual strength into account was used by Ren et al. (Ren et al., 2010) to analyze the debonding of grouted rockbolts. Vaculik et al. (Vaculik et al., 2018) used the same cohesive law to study the full range debonding of FRP-to-substrate joints. Experimental data of PBO FRCM composites reported in (D'Antino et al., 2014) were analyzed via a trilinear cohesive crack model by D'Antino et al. (D'Antino et al., 2018). Two simpler constitutive laws were also used by (Calabrese et al., 2019; Colombi and D'Antino, 2019) to study the same data. Interface damage between FRP and concrete was modeled by (Marfia et al., 2010) through a coupled interface-body nonlocal damage model. Finally, for the pull-push test, a fracture criterion called Finite Fracture Mechanics (FFM) (Cornetti et al., 2006) was utilized by Cornetti et al. (Cornetti et al., 2012) to estimate the delamination load.

2. Mathematical modeling

In order to derive the governing equation of the problem, first, the equilibrium equations for an arbitrary element of the plate as well as for the overall plate and substrate system are needed. Then, assuming the plate and block obey the linear-elastic behavior, we have the governing equation and stress in the plate as follows:

$$\frac{\mathrm{d}^2 s}{\mathrm{d}x^2} - \frac{1+\rho}{E_\mathrm{p}\, h_\mathrm{p}} \tau[s] = 0 \tag{1}$$

$$\sigma[s] = \sigma_\mathrm{p}[s] = \frac{E_\mathrm{p}}{1+\rho} \frac{\mathrm{d}s}{\mathrm{d}x} \tag{2}$$

where ρ= (E_p h_p t_p) / (E_b h_b t_b) and $s = u_p - u_b$. Parameters E_p and E_b illustrate the plate and block Young modulus, h_p and h_b illustrate the plate and block height, while their thickness is shown by t_p and t_b. In Eq. (1), the bond-slip law, $\tau[s]$, is the constitutive (cohesive) law for the interface: in the following two different models are employed.

2.1. Linear Elastic Brittle Interface Model (LEBIM)

According to the LEBIM, the interface is a bed of linear springs with a stiffness equal to k. The constitutive law of the interface is mentioned in Eq. (3):

$$\tau[s] = \begin{cases} k\,s & s \le s_f \\ \tau_r & s > s_f \end{cases} \tag{3}$$

where s_f is the final relative displacement i.e. when the shear stress drops to the residual strength. Considering Fig. 1 and Eq. (2), boundary conditions are:

$$\sigma[0] = 0 \rightarrow s'[0] = 0 \tag{4}$$

$$\sigma[l-a] = \frac{F - \tau_r\, a\, t_p}{t_p\, h_p} \rightarrow s'[l-a] = \frac{1+\rho}{E_p\, t_p\, h_p}\left(F - \tau_r\, a\, t_p\right) \tag{5}$$

where a is the debonded (crack) length with constant stress distribution equal to τ_r. From these boundary conditions, the maximum shear stress is:

$$\tau_{max} = \tau[l-a] = \frac{\sqrt{\mu}}{l_{ch}}\left(\frac{F}{t_p} - a\ \tau_r\right)\coth\left[\frac{l-a}{l_{ch}}\sqrt{\mu}\right] \tag{6}$$

where μ=2 k $\mathcal{G}_{IIc}/\tau_c^2$ and τ_c is the interface strength.

According to Griffith's criterion, propagation occurs as $\mathcal{G}_{II}$ reaches $\mathcal{G}_{IIc}$, hence:

$$\mathcal{G}_{II} = \frac{(\tau_{max} - \tau_r)^2}{2k} = \frac{\left(\frac{\sqrt{\mu}}{l_{ch}}\left(\frac{F}{t_p} - a\ \tau_r\right)\coth\left[\frac{l-a}{l_{ch}}\sqrt{\mu}\right] - \tau_r\right)^2}{2k} = \mathcal{G}_{IIc} \tag{7}$$

Therefore, the debonding load is:

$$\overline{F} = \alpha\overline{\tau}_r + \left(1 + \frac{\overline{\tau}_r}{\sqrt{\mu}}\right)\tanh\left[\left(\lambda - \alpha\right)\sqrt{\mu}\right] \tag{8}$$

where:

$$F_c^{\infty} = t_p\sqrt{\frac{2\,\mathcal{G}_{IIc}\,E_p\,h_p}{1+\rho}}, \quad l_{ch} = \frac{F_c^{\infty}}{\tau_c\,t_p} = \frac{1}{\tau_c}\sqrt{\frac{2\,\mathcal{G}_{IIc}\,E_p\,h_p}{1+\rho}}$$
$$\overline{F} = \frac{F}{F_c^{\infty}}, \quad \lambda = \frac{l}{l_{ch}}, \quad \alpha = \frac{a}{l_{ch}}, \quad \overline{\tau}_r = \frac{\tau_r}{\tau_c} \tag{9}$$

2.2. Maximum load vs. bond length for LEBIM

For bond lengths higher than λ_{lim}=1/$\sqrt{\mu}$ Arccosh[$\sqrt{(\sqrt{\mu}/\tau_r+1)}$], by setting to zero the derivative of the debonding load with respect to the crack length and some mathematical simplification, the maximum load during debonding, F_c, can be calculated as:

$$\overline{F}_c = \frac{F_c}{F_c^{\infty}} = \begin{cases} \left(1+\dfrac{\overline{\tau}_r}{\sqrt{\mu}}\right)\tanh\left[\lambda\sqrt{\mu}\right], & \lambda \le \lambda_{\lim} \\ \overline{\tau}_r\left(\lambda-\lambda_{\lim}\right)+\sqrt{1+\dfrac{\overline{\tau}}{\sqrt{\mu}}}, & \lambda > \lambda_{\lim} \end{cases} \tag{10}$$

2.3. Cohesive crack mode: Rigid-Linear Softening Model (CCM)

According to CCM, the interface is characterized by a linear softening from τ_c to τ_r as the relative displacement s increases from 0 to s_f:

$$\tau[s] = \begin{cases} \tau_c - (\tau_c - \tau_r)\dfrac{s}{s_f} & s \le s_f \\ \tau_r & s > s_f \end{cases} \tag{11}$$

where:

$$s_f = \frac{2\,G_{IIC}}{\tau_c - \tau_r} \tag{12}$$

Using no-slip and traction-free conditions at x=0, $s[0]$=0 and $s'[0]$=0, and employing Eq. (11) for $s < s_f$, the shear stress along the interface is:

$$\tau[x] = \tau_c \cos\left[\frac{x}{l_{ch}}\left(1-\overline{\tau}_r\right)\right] \tag{13}$$

The bond length required for a fully developed softening zone, l_{eff}, can be calculated using the condition of $\tau[l_{eff}] = \tau_r$. Thus:

$$\lambda_{eff} = \frac{l_{eff}}{l_{ch}} = \frac{\mathrm{Arccos}\left[\overline{\tau}_r\right]}{1-\overline{\tau}_r} \tag{14}$$

In Fig. 2, shear stresses for different stages of debonding based on the CCM model are plotted.

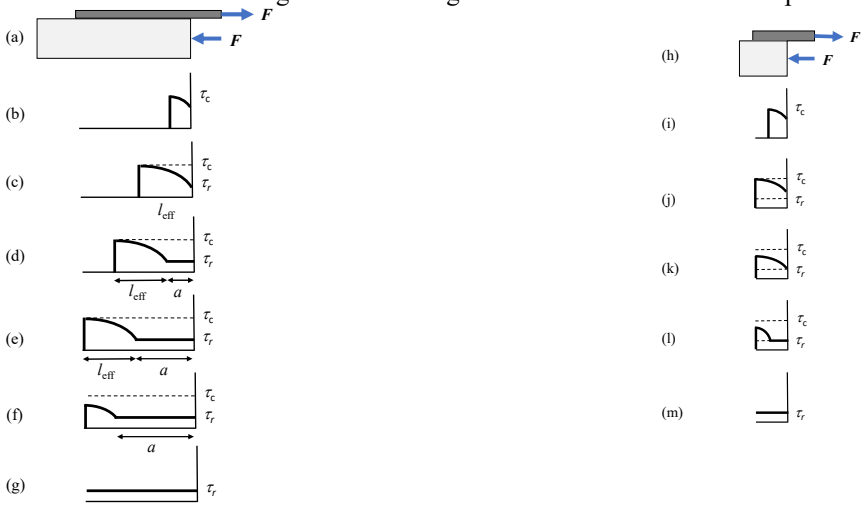

Fig. 2. Distribution of shear stress for different stages of debonding based on the CCM. (a) to (g) for long, and (h) to (m) for short bond lengths.

Debonding load for long bond lengths ($\lambda>\lambda_{\text{eff}}$), (stages (c) to (e)), can be determined as:

$$\overline{F}=\frac{F}{F_{\text{c}}^{\infty}}=\frac{t_{\text{p}}\int_{0}^{l_{\text{eff}}}\tau[x]\,\text{d}x+\tau_{\text{r}}\,a\,t_{\text{p}}}{\tau_{\text{c}}\,l_{\text{ch}}\,t_{\text{p}}}=\frac{\sin\left[\lambda_{\text{eff}}\left(1-\overline{\tau}_{\text{r}}\right)\right]}{1-\overline{\tau}_{\text{r}}}+\overline{\tau}_{\text{r}}\,\alpha,\qquad \alpha<\lambda-\lambda_{\text{eff}} \tag{15}$$

For stages (e) to (g), i.e. $\alpha>\lambda$-λ_{eff}, it is necessary first to solve the governing equation in the softening zone with the first row in Eq. (11) as well as the traction free $s[0]=0$ and $s[l\text{-}a]=s_{\text{f}}$ conditions. Then, we solve the governing equation with the second row in Eq. (11) and continuity conditions of stress and displacement $x = l\text{-}a$. By evaluating the derivative of displacement at the loaded end, we finally get through Eq. (2) the load for stages (e) to (g):

$$\overline{F}=\frac{\overline{\tau}_{\text{r}}}{\left(1-\overline{\tau}_{\text{r}}\right)}\tan\left[\left(\lambda-\alpha\right)\left(1-\overline{\tau}_{\text{r}}\right)\right]+\alpha\,\overline{\tau}_{\text{r}},\qquad \alpha>\lambda-\lambda_{\text{eff}} \tag{16}$$

2.4. Maximum load vs. bond length for CCM:

According to Fig. 2, for short bond lengths, using the stress at stage (j) while for long bond lengths, the stress at stage (e) show the maximum load. Therefore, we have:

$$\overline{F}_{\text{c}}=\frac{F_{\text{c}}}{F_{\text{c}}^{\infty}}=\begin{cases}\dfrac{\sin\left[\lambda\left(1-\overline{\tau}_{\text{r}}\right)\right]}{1-\overline{\tau}_{\text{r}}}, & \lambda\le\lambda_{\text{eff}}\\[2ex] \dfrac{\sin\left[\lambda_{\text{eff}}\left(1-\overline{\tau}_{\text{r}}\right)\right]}{1-\overline{\tau}_{\text{r}}}+\overline{\tau}_{\text{r}}\left(\lambda-\lambda_{\text{eff}}\right), & \lambda>\lambda_{\text{eff}}\end{cases} \tag{17}$$

3. Results and discussions

In this section, the accuracy of equations is evaluated using the debonding load of experimental data available in the Literature, then, a parameter called effective bond length is introduced for the models.

3.1. Available experimental data in the Literature

To compare the accuracy of the models, the maximum debonding loads reported in the Literature (D'Antino et al., 2014) are used for the pull-push test of FRCM-to-concrete joints. The specimens have different bond length of l=100, 150, 200, 250, 330, 450 mm with t_{p} =60mm. Fig. 3 illustrates the predictions of the models vs. the experimental results.

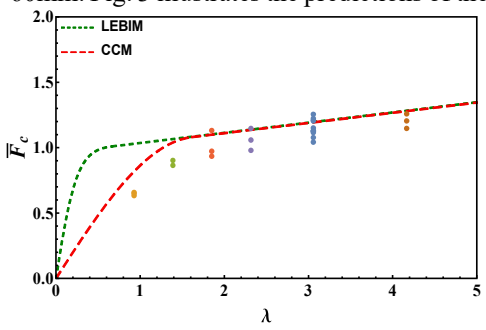

Fig. 3. Predictions of maximum debonding load for LEBIM and CCM.

As shown, estimations are almost the same for long bond lengths and have good consistency with experimental results. However, for short bond lengths, predictions of LEBIM are not accurate enough, while CCM provides good accuracy. Overall, it can be argued that despite the simplicity of equations, models provide good accuracy.

3.2. Effective bond length:

A design parameter called effective bond length can be defined as the length that above it, the load increasing is not significant. For LEBIM, it can be defined as the length that tolerates β percent of the load at the transition point between short and long bond lengths, λ_{lim}, while it is equal to λ_{eff} for CCM. It is worth noting that usually, β= 80-90%. From Fig. 3, it can be said that each model consists of two parts which is separated by λ_{eff}. In the first part, the load increment is significant, while in the second part, it is limited. Effective bond length for LEBIM and CCM can be determined as:

$$\lambda_{eff,LEBIM} = \frac{1}{\sqrt{\mu}} \operatorname{Arctanh}\left[\frac{\beta}{\sqrt{1+\frac{\overline{\tau}_r}{\sqrt{\mu}}}}\right] \tag{18}$$

$$\lambda_{\text{eff,CCM}} = \frac{l_{\text{eff}}}{l_{\text{ch}}} = \frac{\operatorname{Arccos}\left[\overline{\tau}_{\text{r}}\right]}{1-\overline{\tau}_{\text{r}}} \tag{19}$$

4. Conclusions

Two different constitutive interface laws were utilized according to the shear-lag model to study the debonding behavior of composite-to-substrate joints by considering the effect of residual strength. Load variation during the debonding, maximum debonding load and the effective bond length were calculated based on each model in simple closed-form equations. In order to validate the models, the maximum debonding load for both models was calculated against available experimental data in the Literature for the pull-push test. Results illustrated that the CCM model has higher accuracy in predicting the experimental results, especially for short bond lengths, while both models provide almost the same results for long bond lengths. Finally, the effective bond length was determined for each model by considering the effect of residual strength.

Acknowledgements

The funding received from the European Union's Horizon 2020 research and innovation programme under Marie Skłodowska-Curie grant agreement No. 861061- NEWFRAC, "New strategies for multifield fracture problems across scales in heterogeneous systems for Energy, Health and Transport", is gratefully acknowledged.

References

Biscaia, H.C., Borba, I.S., Silva, C., Chastre, C., 2016. A nonlinear analytical model to predict the full-range debonding process of FRP-to-parent material interfaces free of any mechanical anchorage devices. Compos. Struct. 138, 52–63.

Calabrese, A.S., Colombi, P., D'Antino, T., 2019. Analytical solution of the bond behavior of FRCM composites using a rigid-softening cohesive material law. Compos. Part B Eng. 174, 107051. https://doi.org/https://doi.org/10.1016/j.compositesb.2019.107051

Colombi, P., D'Antino, T., 2019. Analytical assessment of the stress-transfer mechanism in FRCM composites. Compos. Struct. 220, 961–970.

Cornetti, P., Carpinteri, A., 2011. Modelling the FRP-concrete delamination by means of an exponential softening law. Eng. Struct. 33, 1988–2001.

Cornetti, P., Mantič, V., Carpinteri, A., 2012. Finite fracture mechanics at elastic interfaces. Int. J. Solids Struct. 49, 1022–1032.

Cornetti, P., Pugno, N., Carpinteri, A., Taylor, D., 2006. Finite fracture mechanics: a coupled stress and energy failure criterion. Eng. Fract. Mech. 73, 2021–2033.

D'Antino, T., Carloni, C., Sneed, L.H., Pellegrino, C., 2014. Matrix-fiber bond behavior in PBO FRCM composites: A fracture mechanics approach. Eng. Fract. Mech. 117, 94–111.

D'Antino, T., Colombi, P., Carloni, C., Sneed, L.H., 2018. Estimation of a matrix-fiber interface cohesive material law in FRCM-concrete joints. Compos. Struct. 193, 103–112. https://doi.org/https://doi.org/10.1016/j.compstruct.2018.03.005

Grande, E., Imbimbo, M., Marfia, S., Sacco, E., 2019. Numerical simulation of the de-bonding phenomenon of FRCM strengthening systems. Frat. ed Integrità Strutt. 47, 321–333.

Marfia, S., Sacco, E., Toti, J., 2010. An approach for the modeling of interface-body coupled nonlocal damage. Frat. ed Integrità Strutt. 4, 13–20.

Muñoz-Reja, M., Cornetti, P., Távara, L., Mantič, V., 2020. Interface crack model using finite fracture mechanics applied to the double pull-push shear test. Int. J. Solids Struct. 188, 56–73.

Ren, F.F., Yang, Z.J., Chen, J.F., Chen, W.W., 2010. An analytical analysis of the full-range behaviour of grouted rockbolts based on a tri-linear bond-slip model. Constr. Build. Mater. 24, 361–370.

Vaculik, J., Sturm, A.B., Visintin, P., Griffith, M.C., 2018. Modelling FRP-to-substrate joints using the bilinear bond-slip rule with allowance for friction—Full-range analytical solutions for long and short bonded lengths. Int. J. Solids Struct. 135, 245–260. https://doi.org/10.1016/j.ijsolstr.2017.11.024

Volkersen, O., 1938. Die Nietkraftverteilung in zugbeanspruchten Nietverbindungen mit konstanten Laschenquerschnitten. Luftfahrtfor schung 15, 41–47.

Yuan, H., Teng, J.G., Seracino, R., Wu, Z.S., Yao, J., 2004. Full-range behavior of FRP-to-concrete bonded joints. Eng. Struct. 26, 553–565.